A joint $\mathcal{H}^2$–$\mathcal{H}^\infty$ algorithm for fading channel estimation and symbol detection

Constantin Siriteanu and Steven D. Blostein
Department of Electrical and Computer Engineering, Queen's University
Kingston, Ontario, Canada, K7L 3N6
E-mail: {costi, sdb}@ee.queensu.ca

Abstract— **This paper proposes a novel recursive method to jointly estimate the Rayleigh fading channel and the transmitted symbols for current wireless communications systems. Starting from the well-known Jakes' model for the wireless fading channel, an autoregressive (AR) representation is produced by the means of Levinson–Durbin algorithm. This allows for a state-space approach to the channel estimation problem, for which the MMSE solution is provided by the celebrated Kalman filter. When the robustness of the estimator is important, the $\mathcal{H}^\infty$ algorithm may be employed instead. It is shown that these algorithms can be combined in order to recover the transmitted symbols and to obtain improved estimates for the envelope and phase of the channel. The paper also proposes a blind channel envelope estimator based on the $\mathcal{H}^\infty$ algorithm.**

I. Introduction

THE demand for mobile wireless communications has increased tremendously in recent years. In the area of digital signal processing for cellular systems, an important research effort is currently focused on finding better methods for estimating the rapidly-changing parameters of the fast fading channel and detecting the high-rate transmitted symbols.

Relatively recently, researchers recognized the performance benefits of the Kalman (also denoted by $\mathcal{H}^2$) and $\mathcal{H}^\infty$ algorithms when applied to wireless communications estimation problems. These algorithms require a state-space model for the random process to be estimated. It is thus necessary to employ an AR or ARMA(AR moving average)-type model to account for the behavior of the actual process. A number of researchers employed AR or ARMA channel models and Kalman recursions to estimate the Rayleigh fading channel [1]–[4]. $\mathcal{H}^\infty$ concepts have also been employed in communications systems for robust equalization [5], beamforming [6] and DOA finding [7].

This paper will show how the $\mathcal{H}^2$ and $\mathcal{H}^\infty$ optimization concepts can be employed to obtain reliable detected symbols and channel estimates.

The structure of the paper is as follows: the next section introduces the Jakes' channel representation of a fading channel and the AR model fitting. Section III outlines the $\mathcal{H}^2$ and $\mathcal{H}^\infty$ estimation criteria and algorithms. In Section IV, a series of observations and theoretical deductions are followed by the main outcome of the paper: a novel method for joint $\mathcal{H}^2$–$\mathcal{H}^\infty$ symbol detection and channel estimation. It is also shown that the $\mathcal{H}^\infty$ algorithm may be used to blindly estimate the envelope of the channel. Simulation results that validate the theoretical deductions are included.

This research was supported by the Canadian Institute for Telecommunications Research under the NCE program of the Government of Canada.

II. Rayleigh fading channel modelling

A. Jakes' model

The work presented in this paper deals with QPSK signals transmitted over a frequency non-selective Rayleigh fading channel for which it employs the well established Jakes' model [10]. Two-dimensional isotropic scattering is assumed and a vertical monopole antenna is employed at the receiver. Suppose that data symbols are transmitted at the rate f_s through this channel. At the k^{th} time sample, the complex channel is:

$$\mathbf{h}_k = \mathbf{h}_{k,I} + \mathrm{j} \cdot \mathbf{h}_{k,Q}, \quad k = 0,\, 1,\, 2,\, \cdots \tag{1}$$

This is assumed to be a WSS Gaussian process, correlated in time, with PSD given by [10]:

$$S_{Jakes}\left(f\right) = \frac{1}{2\pi f_m} \frac{1}{\sqrt{1 - \left(\frac{f}{f_m}\right)^2}} \tag{2}$$

when $f < f_m$, and 0 otherwise; $f_m = f_d/f_s$ is the normalized Doppler frequency. The autocorrelation function for this bandlimited process is:

$$R\left(n\right) = J_0\left(2\pi f_m |n|\right), \tag{3}$$

where $J_0(\cdot)$ is the 0^{th} order Bessel function of the first kind. The simulation results that will appear further in the paper employed the channel generator proposed in [11].

B. AR model fitting

The Yule-Walker equations and the Levinson-Durbin algorithm may be used to fit an AR model of order p to the channel, by minimizing the one-step-ahead prediction mean square error (MSE), as in [12]. The AR(p) model for the channel is:

$$\mathbf{h}_{k+1} = -a_1 \mathbf{h}_k \ldots - a_p \mathbf{h}_{k-(p-1)} + \mathbf{w}_k, \tag{4}$$

where $\mathbf{w}_k$ is a zero-mean complex white Gaussian noise, with variance $\sigma^2_{\mathbf{w}}$. The PSD of this process is obviously given by:

$$S_{AR}(f) = \frac{\sigma^2_{\mathbf{w}}}{\left|1 + \sum_{l=1}^{p} a_l \cdot e^{-2\pi \mathrm{j} f l}\right|^2}. \tag{5}$$

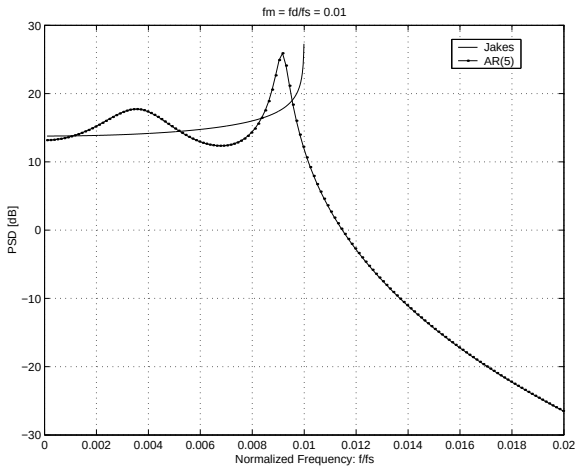

Fig. 1. PSD for Jakes' model and fitted AR(5) process.

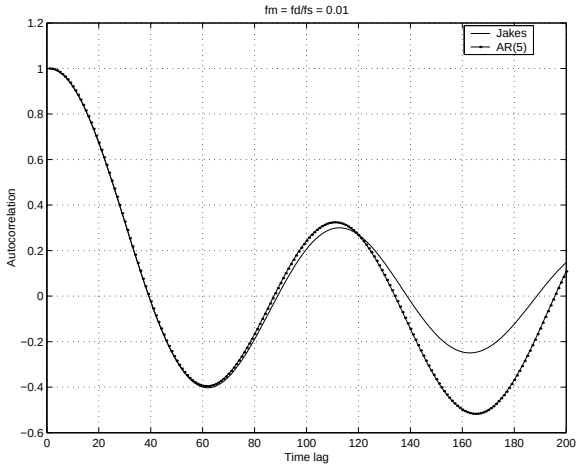

Fig. 2. Autocorrelation for Jakes' model and fitted AR(5) process.

Figure 1 shows the comparison between PSDs for the Jakes' model and the fitted AR(5) model when $f_s = 10\ KHz$ and $f_d = 100\ Hz$ (thus, $f_m = 0.01$). Figure 2 shows the autocorrelation comparison. These figures suggest that fitting an AR(5) model for the Jakes' Rayleigh fading channel provides relatively close PSD and autocorrelation match. Actually, it can be shown that the prediction MSE (variance of $\mathbf{w}_k$) decreases with the increase of the chosen process order [12]. Therefore, increasing the AR model order necessarily leads to a better fit of the resulting process on the true Jakes' channel. However, the higher the chosen AR model order, the more computationally complex and numerically unstable will be the estimation algorithms presented in further sections. A compromise is always necessary, and, therefore, an AR(5) model was chosen to obtain the simulation results presented later in the paper.

C. State-space representation

Suppose that the Rayleigh fading channel has been modelled as an AR(p) process (see Equation (4)). A very simple model for the received signal is adopted:

$$\mathbf{y}_k = s_k \cdot \mathbf{h}_k + \mathbf{v}_k, \tag{6}$$

where $s_k = e^{\mathrm{j}\{\pm\pi/4,\, \pm 3\pi/4\}}$ is the transmitted QPSK symbol. Assume that $\mathbf{w}_k$ in (4) and $\mathbf{v}_k$ in (6) are white zero-mean Gaussian noises with variances given by $\mathbf{Q}_k$ (denoted by $\sigma^2_{\mathbf{w}}$ in Section II) and $\mathbf{R}_k$, respectively. The above equations can be re-written in the following state-space form:

$$\begin{aligned} \underline{\mathbf{h}}_{k+1} &= \mathbf{F}_k \cdot \underline{\mathbf{h}}_k + \mathbf{G}_k \cdot \mathbf{w}_k & (7)\\ \mathbf{y}_k &= \mathbf{H}_k \cdot \underline{\mathbf{h}}_k + \mathbf{v}_k. & (8) \end{aligned}$$

where

$$\underline{\mathbf{h}}_k = \begin{bmatrix} \mathbf{h}_k \\ \mathbf{h}_{k-1} \\ \vdots \\ \mathbf{h}_{k-(p-1)} \end{bmatrix} \quad \mathbf{F}_k = \begin{bmatrix} -a_1 & -a_2 & \cdots & -a_p \\ 1 & 0 & \cdots & 0 \\ \vdots & \vdots & \cdots & \vdots \\ 0 & 0 & \cdots & 0 \end{bmatrix}_{p\times p}$$

$$\mathbf{H}_k = [s_k\ 0\ \cdots\ 0]_{1\times p} \quad \text{and} \quad \mathbf{G}_k = [1\ 0\ \cdots\ 0]^T_{1\times p}.$$

III. $\mathcal{H}^2$ and $\mathcal{H}^\infty$ estimation algorithms

The issue of estimation for the system described by (7) and (8) can now be approached with $\mathcal{H}^2$ and $\mathcal{H}^\infty$ methods: the former, a stochastic approach, minimizes the estimation MSE; the latter, a deterministic approach, minimizes (in the optimal case) or bounds (in the suboptimal case) the worst-case estimation error. In general, a linear combination of the states has to be estimated:

$$\mathbf{c}_{k+1} = \mathbf{L}_{k+1} \cdot \underline{\mathbf{h}}_{k+1}$$

The $\mathcal{H}^2$ estimation problem: find a linear estimation strategy $\hat{\mathbf{c}}_{k+1|k+1} = g(\mathbf{y}_0, \mathbf{y}_1, \cdots, \mathbf{y}_{k+1})$ that minimizes:

$$E \sum_{j=0}^{k+1} \left(\mathbf{c}_j - \hat{\mathbf{c}}_{j|j}\right)^H \cdot \left(\mathbf{c}_j - \hat{\mathbf{c}}_{j|j}\right), \tag{9}$$

where E stands for statistical mean.

Solution (the celebrated Kalman filter): the optimum estimate is given by $\hat{\mathbf{c}}_{k+1|k+1} = \mathbf{L}_{k+1} \cdot \hat{\underline{\mathbf{h}}}_{k+1|k+1}$, while the state vector estimate satisfies the following recursions [9]:

$$\begin{aligned} \hat{\underline{\mathbf{h}}}_{k+1|k} &= \mathbf{F}_k \hat{\underline{\mathbf{h}}}_{k|k} & (10)\\ \hat{\underline{\mathbf{h}}}_{k+1|k+1} &= \hat{\underline{\mathbf{h}}}_{k+1|k} + \\ &\quad \mathbf{K}_{k+1}\left(\mathbf{y}_{k+1} - \mathbf{H}_{k+1}\hat{\underline{\mathbf{h}}}_{k+1|k}\right) & (11)\\ \mathbf{K}_{k+1} &= \mathbf{P}_{k+1}\mathbf{H}^H_{k+1}\mathbf{R}^{-1}_{e,k+1} & (12)\\ \mathbf{P}_{k+1} &= \mathbf{F}_k\mathbf{P}_k\mathbf{F}^H_k + \mathbf{G}_k\mathbf{Q}_k\mathbf{G}^H_k - \\ &\quad \mathbf{F}_k\mathbf{P}_k\mathbf{H}^H_k\mathbf{R}^{-1}_{e,k}\mathbf{H}_k\mathbf{P}_k\mathbf{F}^H_k & (13)\\ \mathbf{R}_{e,k} &= \mathbf{R}_k + \mathbf{H}_k\mathbf{P}_k\mathbf{H}^H_k, & (14) \end{aligned}$$

and $\hat{\underline{\mathbf{h}}}_{0|0}$ and $\mathbf{P}_0$ are specified at start-up.

The $\mathcal{H}^\infty$ suboptimal estimation problem: given γ, find a linear estimation strategy $\hat{\mathbf{c}}_{k+1|k+1} = g(\mathbf{y}_0, \mathbf{y}_1, \cdots, \mathbf{y}_{k+1})$ such that the maximum value of the error energy gain

$$\frac{\sum_{j=0}^{k+1} \left(\mathbf{c}_j - \hat{\mathbf{c}}_{j|j}\right)^H \cdot \left(\mathbf{c}_j - \hat{\mathbf{c}}_{j|j}\right)}{\left(\underline{\mathbf{h}}_0 - \hat{\underline{\mathbf{h}}}_{0|0}\right)^H \Pi_0^{-1} \left(\underline{\mathbf{h}}_0 - \hat{\underline{\mathbf{h}}}_{0|0}\right) + \sum_{j=0}^{k+1} \left(\mathbf{w}_j^H \mathbf{w}_j + \mathbf{v}_j^H \mathbf{v}_j\right)} \tag{15}$$

is less than γ^2 for all possible $\underline{\mathbf{h}}_0$, $\{\mathbf{w}_j\}_0^{k+1}$, $\{\mathbf{v}_j\}_0^{k+1}$. Note that in this case, unlike for the Kalman algorithm, the initial estimation error is accounted for with the weighting matrix Π_0^{-1}.

Solution: if $[\mathbf{F}_j\, \mathbf{G}_j]$ are full-rank matrices for any $j = 1, \cdots, k$, then a solution to the above problem exists if and only if the following positivity condition holds:

$$\mathbf{P}_j^{-1} + \mathbf{H}_j^H \mathbf{H}_j - \gamma^{-2} \mathbf{L}_j^H \mathbf{L}_j > 0, \quad j = 1, \cdots, k. \tag{16}$$

The *central* $\mathcal{H}^\infty$ estimate is given by $\hat{\mathbf{c}}_{k+1|k+1} = \mathbf{L}_{k+1} \cdot \hat{\underline{\mathbf{h}}}_{k+1|k+1}$, while the state vector estimate satisfies the following recursions [9]:

$$\hat{\underline{\mathbf{h}}}_{k+1|k} = \mathbf{F}_k \hat{\underline{\mathbf{h}}}_{k|k} \tag{17}$$

$$\hat{\underline{\mathbf{h}}}_{k+1|k+1} = \hat{\underline{\mathbf{h}}}_{k+1|k} + \mathbf{K}_{k+1} \left(\mathbf{y}_{k+1} - \mathbf{H}_{k+1} \hat{\underline{\mathbf{h}}}_{k+1|k}\right) \tag{18}$$

$$\mathbf{K}_{k+1} = \mathbf{P}_{k+1} \mathbf{H}_{k+1}^H \left(\mathbf{I} + \mathbf{H}_{k+1} \mathbf{P}_{k+1} \mathbf{H}_{k+1}^H\right)^{-1} \tag{19}$$

$$\mathbf{P}_{k+1} = \mathbf{F}_k \mathbf{P}_k \mathbf{F}_k^H + \mathbf{G}_k \mathbf{G}_k^H - \mathbf{F}_k \mathbf{P}_k \left[\mathbf{H}_k^H\, \mathbf{L}_k^H\right] \mathbf{R}_{e,k}^{-1} \begin{bmatrix} \mathbf{H}_k \\ \mathbf{L}_k \end{bmatrix} \mathbf{P}_k \mathbf{F}_k^H \tag{20}$$

$$\mathbf{R}_{e,k} = \begin{bmatrix} \mathbf{I} & \mathbf{0} \\ \mathbf{0} & -\gamma^2 \mathbf{I} \end{bmatrix} + \begin{bmatrix} \mathbf{H}_k \\ \mathbf{L}_k \end{bmatrix} \mathbf{P}_k \left[\mathbf{H}_k^H\, \mathbf{L}_k^H\right] \tag{21}$$

where $\hat{\underline{\mathbf{h}}}_{0|0}$ and $\mathbf{P}_0 = \Pi_0$ are given at start-up.

Note the differences between the $\mathcal{H}^2$ and $\mathcal{H}^\infty$ methods: no statistical information about the noises is necessary for the $\mathcal{H}^\infty$ algorithm; moreover, the matrix $\mathbf{L}_k$ enters the recursions for the $\mathcal{H}^\infty$ channel estimate.

IV. Employing $\mathcal{H}^2$ and $\mathcal{H}^\infty$ criteria for channel estimation and symbol detection

A. Effects of an incorrect symbol on channel estimation

For the same system parameters (f_s and f_d) as in II-B, the $\mathcal{H}^2$ and $\mathcal{H}^\infty$ estimation algorithms described in Section III have been employed to estimate the envelope and phase of $\mathbf{h}_{k+1} = |\mathbf{h}_{k+1}| \cdot e^{\mathrm{j} \cdot \psi_{k+1}}$. Moreover, a decision feedback error has been introduced: the matrix $\mathbf{H}_{k+1}$ used in the algorithms contains a certain detected symbol, $\hat{s}_{k+1}$; this symbol does not coincide with s_{k+1} from $\mathbf{H}_{k+1}$ in the measurement equation (6). Figures 3 and 4 describe how using an incorrect symbol in the $\mathcal{H}^2$ and $\mathcal{H}^\infty$ estimation algorithms reflects upon the quality of the estimates.

Observations:

- While the $\mathcal{H}^\infty$ estimate of the envelope behaves as if no error were introduced, the estimate of the phase shows an important deviation from the true value. However, when the error disappears, the phase of the estimate immediately returns to the nominal behavior, i.e., the behavior when correct symbols are used in the algorithm.
- The Kalman estimate of the envelope shows a significantly large deviation. Moreover, the estimate returns to the nominal behavior only after a long transitory period.

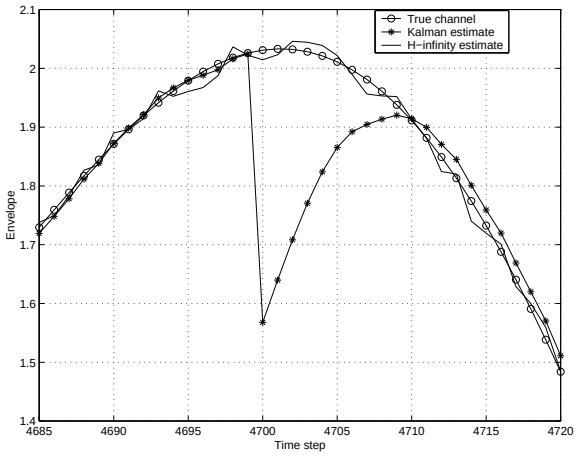

Fig. 3. Symbol error effect on envelope estimates

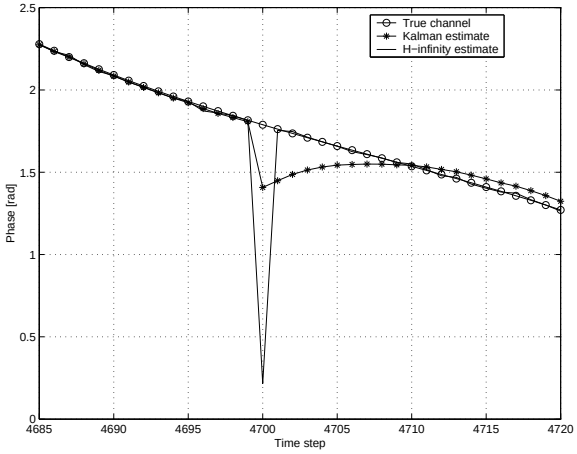

Fig. 4. Symbol error effect on phase estimates

These observations lead to the conclusion that the $\mathcal{H}^\infty$ algorithm provides a better channel envelope estimate than its $\mathcal{H}^2$ counterpart. This is shown to be true by the simulations described later in IV-D.

B. Theoretical explanation

The underlying reasons for the behavior described in IV-A are analyzed next. The relation between the true (transmitted) symbol and the symbol used in the estimation algorithms may be stated as:

$$\hat{s}_{k+1} = e^{\mathrm{j}\Delta\psi_{k+1}} \cdot s_{k+1}. \tag{22}$$

Define:

$$\Delta \hat{\underline{\mathbf{h}}}_{k|k} = e^{-\mathrm{j}\Delta\psi_k} \cdot \hat{\underline{\mathbf{h}}}_k - \hat{\underline{\mathbf{h}}}_{k|k}. \tag{23}$$

Neglecting the noises $\mathbf{w}_k$ in (7) and $\mathbf{v}_k$ in (8), and using the recursions from Section III, it can be shown that, for

both algorithms, the following approximation holds:

$$\Delta\underline{\hat{\mathbf{h}}}_{k+1|k+1} \approx \left(\mathbf{I} - \mathbf{P}_{k+1}\mathbf{H}_{k+1}^H\mathbf{R}_{e,k+1}^{-1}\mathbf{H}_{k+1}\right)\mathbf{F}_k\Delta\underline{\hat{\mathbf{h}}}_{k|k} \tag{24}$$

Using results from [13] and [14], it can be shown that the elements of the matrix $\mathbf{P}_{k+1}$ are bounded for the Kalman case, while permanently increasing and unbounded for the $\mathcal{H}^\infty$ case. In Equation (24) the matrix $\mathbf{P}_{k+1}$ multiplies the *inverse* of $\mathbf{R}_{e,k+1}$, which also depends on $\mathbf{P}_{k+1}$, as in Equations (14) and (21), where k is replaced by $k+1$. Furthermore, the biased Levinson–Durbin algorithm discussed in II-B leads to a stable matrix $\mathbf{F}_k$. It can be proved that, after a sufficient number of time steps, the following holds for the Kalman algorithm:

$$e^{-\mathrm{j}\Delta\psi_{k+1}}\cdot\mathbf{h}_{k+1} - \hat{\mathbf{h}}_{k+1|k+1}^{\mathcal{H}^2} \approx const\cdot\left(\mathbf{h}_k - e^{\mathrm{j}\Delta\psi_{k+1}}\cdot\hat{\mathbf{h}}_{k|k}^{\mathcal{H}^2}\right), \tag{25}$$

while for the $\mathcal{H}^\infty$ algorithm:

$$e^{-\mathrm{j}\Delta\psi_{k+1}}\cdot\mathbf{h}_{k+1} - \hat{\mathbf{h}}_{k+1|k+1}^{\mathcal{H}^\infty} \approx 0. \tag{26}$$

The reasons for the behavior described in IV-A are now obvious.

Relations (25) and (26) are direct consequences of the facts that the upper bound on the error energy gain is very close to unity for $\mathcal{H}^\infty$ [14], while the intrinsic value of this bound is much higher for $\mathcal{H}^2$ [9]. These relations also suggest what is well known in the robust estimation literature: the performance of the $\mathcal{H}^\infty$ estimator depends much less on the choice of the channel model than the Kalman estimator.

C. Proposed method

A novel method for symbol detection and channel estimation is proposed next. If Equation (25) is subtracted from Equation (26), and the variance operator is applied to both sides, the following is obtained:

$$E\left|\hat{\mathbf{h}}_{k+1|k+1}^{\mathcal{H}^2} - \hat{\mathbf{h}}_{k+1|k+1}^{\mathcal{H}^\infty}\right|^2 \approx const\cdot E\left|\mathbf{h}_k - e^{\mathrm{j}\Delta\psi_{k+1}}\cdot\hat{\mathbf{h}}_{k|k}^{\mathcal{H}^2}\right|^2. \tag{27}$$

Obviously, $\hat{\mathbf{h}}_{k|k}^{\mathcal{H}^2}$ minimizes $E\left|\mathbf{h}_k - \hat{\mathbf{h}}_{k|k}\right|^2$. Then:

$$E\left|\mathbf{h}_k - e^{\mathrm{j}\Delta\psi_{k+1}}\cdot\hat{\mathbf{h}}_{k|k}^{\mathcal{H}^2}\right|^2 \geq E\left|\mathbf{h}_k - \hat{\mathbf{h}}_{k|k}^{\mathcal{H}^2}\right|^2 \tag{28}$$

holds for any value of $\Delta\psi_{k+1}$, and is satisfied with equality for $\Delta\psi_{k+1} = 0$. Equations (27) and (28) lead to:

$$E\left|\hat{\mathbf{h}}_{k+1|k+1}^{\mathcal{H}^2} - \hat{\mathbf{h}}_{k+1|k+1}^{\mathcal{H}^\infty}\right|^2 \geq$$

$$E\left|\hat{\mathbf{h}}_{k+1|k+1}^{\mathcal{H}^2} - \hat{\mathbf{h}}_{k+1|k+1}^{\mathcal{H}^\infty}\right|^2_{\Delta\psi_{k+1}=0}. \tag{29}$$

Therefore, the mean square difference between the state estimates provided by the $\mathcal{H}^2$ and $\mathcal{H}^\infty$ algorithms is minimized when the correct (transmitted) symbol is used, i.e., $\Delta\psi_{k+1} = 0$.

Thus motivated, the proposed (further denoted as *joint* $\mathcal{H}^2$–$\mathcal{H}^\infty$) algorithm for symbol recovery and channel estimation is outlined next:

1. Initial training period: initialize both Kalman and $\mathcal{H}^\infty$ algorithms and run them a long enough training period so that (25) and (26) hold.
2. Normal operating period (employs periodic training symbols):
   (a) for each possible constellation symbol, execute both Kalman and $\mathcal{H}^\infty$ algorithms and determine the channel estimates; then, find the absolute value of the difference between the two estimates;
   (b) the detected symbol will be the one that produces the minimum value at the previous step;
   (c) the corresponding channel estimate provided by the Kalman algorithm is considered.

D. Simulation results

Performance of the proposed method

An alternative procedure for joint channel estimation and symbol detection was used to provide a means of performance comparison for the algorithm proposed in IV-C. The basic recursions from Section III are modified as in [8] in order to transform the Kalman and $\mathcal{H}^\infty$ algorithms into decision–directed estimation procedures:

1. From step k: $\hat{\mathbf{h}}_{k|k}$ is known and the *a priori* channel estimate $\hat{\mathbf{h}}_{k+1|k} = \mathbf{F}_k\hat{\mathbf{h}}_{k|k}$ can be calculated.
2. At step $k+1$:
   (a) take the new measurement, i.e., $\mathbf{y}_{k+1}$
   (b) determine the constellation symbol closest to $\mathbf{y}_{k+1}/\hat{\mathbf{h}}_{k+1|k}$
   (c) use this "predicted" symbol in the algorithms to determine the *a posteriori* channel estimate $\hat{\mathbf{h}}_{k+1|k+1}$
   (d) determine the constellation symbol closest to $\mathbf{y}_{k+1}/\hat{\mathbf{h}}_{k+1|k+1}$; consider this to be the detected symbol and use it for the next iteration, in the matrix $\mathbf{H}_k$, when updating from $\mathbf{P}_k$ to $\mathbf{P}_{k+1}$ in equations (13) and (20).

The performance of the joint $\mathcal{H}^2$–$\mathcal{H}^\infty$ algorithm is compared to the decision–directed $\mathcal{H}^\infty$ and Kalman algorithms in Figures 5 and 6 for symbol error rate (SER) and mean square error (MSE), respectively. For the Kalman algorithm 2 training symbols in 10 were used because for 1/10 the results are much worse than for the other algorithms. Clearly, the proposed method performs better than the two decision–directed alternatives. The MSE performance of the Kalman decision-directed algorithm approaches the performance of the proposed algorithm as the SNR increases. The reason is that the channel estimate for the joint $\mathcal{H}^2$–$\mathcal{H}^\infty$ algorithm is also given by a Kalman algorithm: however, the symbol used in the algorithm is detected using the proposed method instead of the one from [8]. As the SNR increases, the SER decreases for both the joint $\mathcal{H}^2$–$\mathcal{H}^\infty$ and the decision–directed Kalman algorithm, and therefore, asymptotically, the MSE values should become equal.

The joint $\mathcal{H}^2$–$\mathcal{H}^\infty$ algorithm is highly parallelizable and, therefore, its computation time per update will approxi-

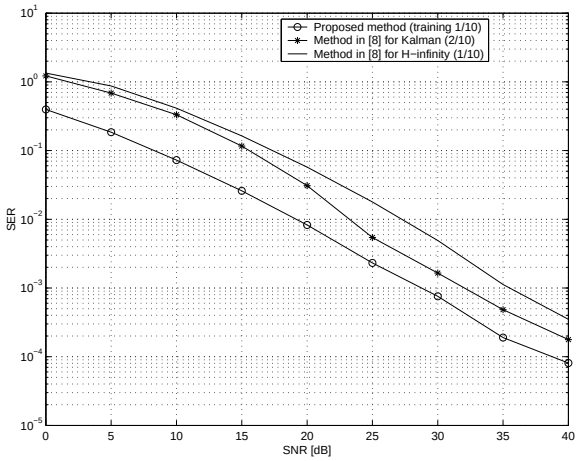

Fig. 5. SER performance for proposed and decision-directed methods

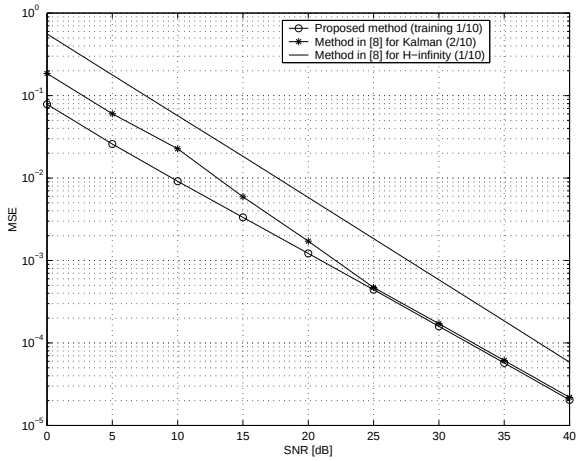

Fig. 6. MSE performance for proposed and decision-directed methods

mately be the same as for the described decision–directed algorithms.

Blind channel envelope estimation

In the context of the observations from IV-A, an experimental study of the blind $\mathcal{H}^2$ and $\mathcal{H}^\infty$ channel envelope estimation was done. The symbol $\hat{s}_{k+1}$ used in matrix $\mathbf{H}_{k+1}$ in the recursions was chosen randomly. A qualitative comparison between the blind $\mathcal{H}^2$ and $\mathcal{H}^\infty$ envelope estimators for SNR = 30 dB is presented in Figure 7. Notice that, while the Kalman algorithm fails to blindly estimate the channel envelope, the $\mathcal{H}^\infty$ algorithm yields an estimate consistent with the perfect decision-feedback case.

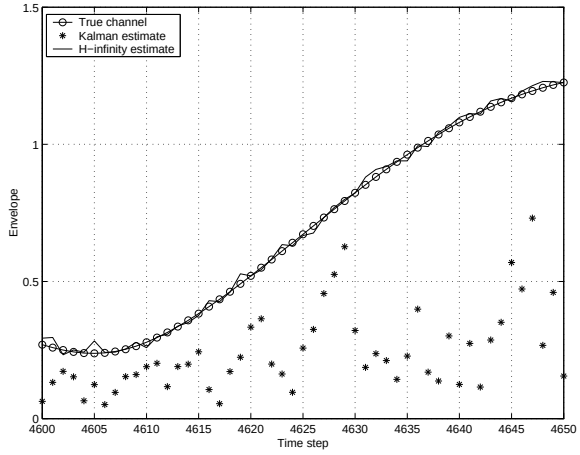

Fig. 7. Comparison of blind $\mathcal{H}^\infty$ and $\mathcal{H}^2$ envelope estimates

V. Conclusions

The paper proposes a novel procedure for joint symbol detection and fading channel estimation. The method exploits joint $\mathcal{H}^2$ and $\mathcal{H}^\infty$ optimization criteria, and the symbol that minimizes the (mean) distance between the Kalman and $\mathcal{H}^\infty$ estimators is proved to be the true (transmitted) symbol. Simulation results show that the performance of this method compares very well to another decision–directed channel estimation method. The paper also shows that the $\mathcal{H}^\infty$ algorithm, unlike its $\mathcal{H}^2$ counterpart, can be employed to produce a blind estimate for the envelope of the fading channel.

References

[1] Iltis, R. A., "Joint estimation of PN code delay and multipath using the extended Kalman filter", *IEEE Transactions on Communications*, vol. 38, no. 10, pp. 1677-1685, Oct. 1990.

[2] Ma, Y. and Lim, T. J., "Linear and nonlinear chip-rate MMSE multiuser CDMA detection", *IEEE Transactions on Communications*, vol. 49, no. 3, pp. 530-542, Mar. 2001.

[3] Tsatsanis, M. K., Giannakis, G. B., Zhou, G., "Estimation and equalization of fading channels with random coefficients", Elsevier: *Signal Processing*, vol. 53, pp. 211-229, 1996.

[4] Chen, L.-M. and Chen, B.-S., "A robust adaptive DFE receiver for DS–CDMA systems under multipath fading channels", *IEEE Transactions on Signal Processing*, vol. 49, no. 7, pp. 1523–1532, July 2001.

[5] Erdogan, A. T., "Equalization with an $\mathcal{H}^\infty$ criterion", Ph. D. thesis, Stanford University, 1999.

[6] Ratnarajah, T. and Manikas, A., "A robust signal-copy beamformer using $\mathcal{H}^\infty$ estimation", *IEEE Proceedings of the* 30^{th} *Asilomar Conference on Signals, Systems and Computers*, Pacific Grove, CA, pp. 551–555, Nov. 1996.

[7] Ratnarajah, T. and Manikas, A., "An $\mathcal{H}^\infty$ approach to mitigate the effects of array uncertainties on the MuSIC algorithm", *IEEE Signal Processing Letters*, vol. 5, no. 7, pp. 185–188, July 1998.

[8] Liu, Z., Ma, X. and Giannakis, G. B., "Space-time coding and Kalman filtering for time-selective fading channels", *IEEE Transactions on Communications*, vol. 50, no. 2, pp. 183–186, Feb. 2002.

[9] Hassibi, B., Sayed, A. H. and Kailath, T., *Indefinite-quadratic estimation and control. A unified approach to* $\mathcal{H}^2$ *and* $\mathcal{H}^\infty$ *theories*, SIAM, 1999.

[10] Jakes, W. C., *Microwave Mobile Communications*, New York: Wiley, 1994.

[11] Young, D. J., "The generation of correlated Rayleigh random variates by DFT and quality measures for random variate generation", Master's thesis, Queen's University, Kingston, Canada, 1997.

[12] Baddour, K. E. and Beaulieu, N. C., "Autoregressive models for fading channel simulations", in *Proc. IEEE Globecom'01*, San Antonio, TX, pp. 1187-1192, Nov. 2001.

[13] Anderson, B. D. O. and Moore, J. B., *Optimal Filtering*, Prentice-Hall, 1979.

[14] Bolzern, P., Colaneri, P. and de Nicolao, G., "$\mathcal{H}^\infty$-robustness of adaptive filters against measurement noise and parameter drift", *Automatica*, vol. 35, pp. 1509-1520, 1999.